ACS chemical biology

Articles

pubs.acs.org/acschemicalbiology

Identification of Drug Modulators Targeting Gene-Dosage Disease CMT1A

Sung-Wook Jang,[†] Camila Lopez-Anido,[§] Ryan MacArthur,[†] John Svaren,[§] and James Inglese*[,†,‡]

[†]National Center of Advancing Translational Sciences and [‡]National Human Genome Research Institute, National Institutes of Health, Bethesda, Maryland 20892, United States

[§]Department of Comparative Biosciences, and Waisman Center, University of Wisconsin, Madison, Wisconsin 53705, United States

Supporting Information

ABSTRACT: The structural integrity of myelin formed by Schwann cells in the peripheral nervous system (PNS) is required for proper nerve conduction and is dependent on adequate expression of myelin genes including peripheral myelin protein 22 (*PMP22*). Consequently, excess PMP22 resulting from its genetic duplication and overexpression has been directly associated with the peripheral neuropathy called Charcot-Marie-Tooth disease type 1A (CMT1A), the most prevalent type of CMT. Here, in an attempt to identify transcriptional inhibitors with therapeutic value toward CMT1A, we developed a cross-validating pair of orthogonal reporter assays, firefly luciferase (FLuc) and β-lactamase (βLac), capable of recapitulating PMP22 expression, utilizing the intronic regulatory element of the human *PMP22* gene. Each compound from a collection of approximately 3,000 approved drugs was tested at multiple titration points to achieve a pharmacological end point in a 1536-well plate quantitative high-throughput screen (qHTS) format. In conjunction with an independent counter-screen for cytotoxicity, the design of our orthogonal screen platform effectively contributed to selection and prioritization of active compounds, among which three drugs (fenretinide, olvanil, and bortezomib) exhibited marked reduction of endogenous Pmp22 mRNA and protein. Overall, the findings of this study provide a strategic approach to assay development for gene-dosage diseases such as CMT1A.

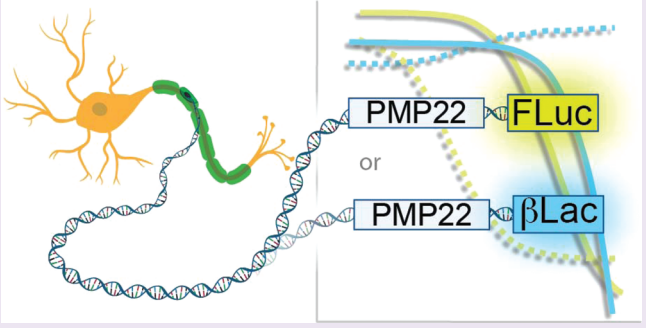

The formation of myelin sheath around axons by Schwann cells, a process known as myelination, is a critical component of peripheral nervous system (PNS) postnatal development in vertebrates. The lipid-rich myelin sheath supports axonal stability and enables rapid, saltatory propagation of action potentials.[1] Disruption of myelin structure by genetic factors has been recognized as a main cause of human peripheral neuropathies such as Charcot-Marie-Tooth (CMT) disease. Over the past two decades, molecular genetics research has identified over 30 genes whose alterations are associated with the CMT phenotypes including peripheral myelin protein 22 (*PMP22*).[2]

The *PMP22* gene encodes a small tetraspan 22-kDa membrane glycoprotein that plays an essential role in myelin synthesis and assembly, representing 2−5% of PNS myelin proteins.[1] The elevated gene-dosage derived from the duplication of the *PMP22* gene has been shown to be culpable for pathological hallmarks of CMT type 1A (CMT1A), a predominant type of CMT.[3] Typical symptoms of CMT1A include distal muscle atrophy, sensory loss, hyporeflexia, and skeletal deformity. On the other hand, the haploinsufficiency of *PMP22* by its reciprocal deletion is associated with a distinct neurological disorder called hereditary neuropathy with liability to pressure palsies (HNPP).[4] Despite the concomitant genetic occurrence, HNPP is less prevalent than CMT1A due to its mild, transient symptoms that render the disease unnoticed or misdiagnosed. The fact that a moderate change in expression by its altered copy number leads to clinical phenotypes indicates that PMP22 levels must be tightly controlled to ensure proper myelination by Schwann cells. Previous transgenic studies have revealed regulatory elements that direct spatial and temporal expression of PMP22.[5,6] Whereas an upstream region (−10 to −6.5 kb) is sufficient to activate reporter expression only at later stages of PNS development and is thus named the late myelination Schwann cell-specific element (LMSE), a recently discovered intronic element at +11 kb was found to mediate at least part of the induction of PMP22 during myelination.

Studies in rodent models of CMT1A have identified two transcription-based strategies that ameliorate the disease by reducing levels of Pmp22. The first is high dose ascorbic acid, which has formed the basis of the only current clinical trial of CMT1A.[7] The effects of ascorbic acid may be diverse, but one aspect of its function appears to be reduction in cAMP signaling.[8] Unfortunately, the early results of the human clinical

Received: February 1, 2012
Accepted: April 25, 2012
Published: April 25, 2012

   dx.doi.org/10.1021/cb300048d | *ACS Chem. Biol.* 2012, 7, 1205−1213

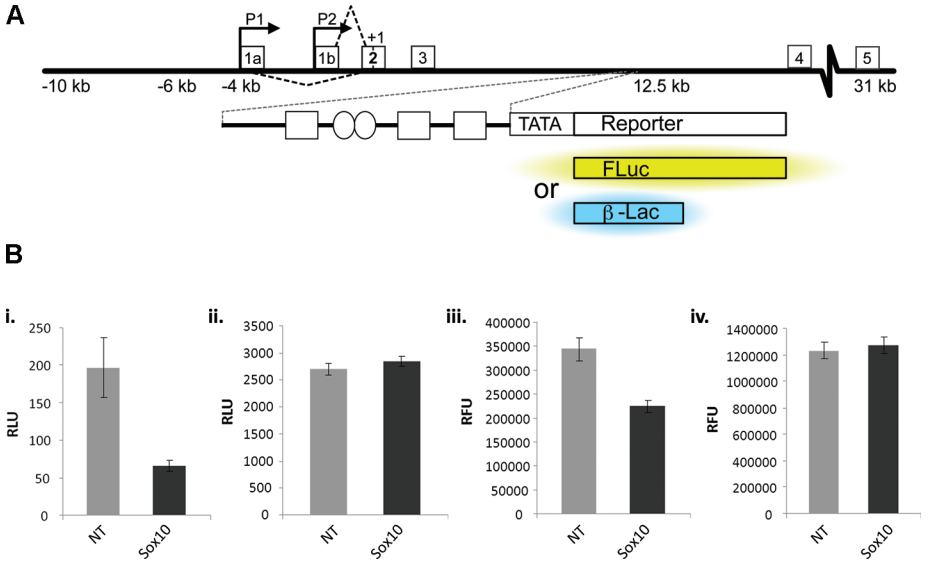

Figure 1. Assay design and validation. (A) A schematic diagram of reporter constructs derived from the intronic element of the human *PMP22* locus. Dimeric Sox10 binding site and Egr2 binding sites are represented by ovals and boxes, respectively. (B) siRNA-induced depletion of Sox10 leads to downregulation of both the Fluc and *β*Lac reporters without affecting cell viability. The reporter (FLuc or *β*Lac) expressing S16 cells was treated with Sox10-siRNA or NT (nontargeting)-siRNA as a control for 48 h. Whereas the FLuc cells were subjected to luciferase assay (i) for FLuc expression or CellTiter-Glo assay (ii) for viability, the *β*Lac cells were processed for *β*Lac expression (iii) and viability (iv) measured at 460 and 535 nm, respectively. Error bars indicate the SD of replicates (n = 144 for the FLuc cells, n = 192 for the *β*Lac cells).

trial have so far not revealed a significant effect in CMT1A patients, although the final results of these trials are yet to emerge.[9] In addition, proof-of-principle studies using progesterone antagonists to reduce Pmp22 expression in a rat model of CMT1A have shown beneficial effects.[10] These studies demonstrate that a relatively subtle (<2-fold) change in PMP22 transcription could effectively treat the most common form of inherited peripheral neuropathy.

There is great potential for pharmacological intervention to downregulate PMP22 levels for a treatment of CMT1A, especially since clinical tolerance for excess reduction of PMP22 in CMT1A patients is reflected in mild symptoms of HNPP relative to those of CMT1A. However, one of the major limitations in therapeutic research for CMT1A has been the lack of viable assay systems that can broadly and effectively screen small molecules for their biological relevance to CMT1A. Here, we describe the development of transcription-based cellular assays amenable to quantitative high-throughput screen (qHTS) to identify PMP22-modulating chemical agents, representing the first application of HTS to the translational therapeutic efforts aimed at CMT1A.

RESULTS AND DISCUSSION

Development of an Orthogonal Pair of Transcription-Based Assays. A recent study has indicated that tissue-specific expression of PMP22 is governed in part by the regulatory element residing in the largest intron of the *PMP22* gene, which is activated by transcription factors Egr2 and Sox10, the master regulators of PNS myelination.[6] In an attempt to identify chemical agents capable of downregulating PMP22, we utilized the intronic element to develop transcription-based reporter assays to be used as a cell-sensor for PMP22 expression (Figure 1A). A pair of primary cross-validating assays was established with the intronic element conjugated to drive either firefly luciferase (FLuc) or *β*-lactamase (*β*Lac) expression, which was stably transfected into S16 rat Schwann cells previously shown to sustain high levels of Pmp22 expression comparable to those in myelinating Schwann cells.[11] Establishment of an assay platform in human cellular context was hindered by unavailability of human-derived Schwann cell lines expressing physiological levels of PMP22. The use of the orthogonal assays allowed discrimination against nonspecific activity intrinsic to either FLuc or *β*Lac reporters themselves. The bioluminescent FLuc signal is complemented by the dual *β*Lac output composed of fluorescence at 460 nm for *β*Lac expression and FRET at 535 nm for cell viability.[12] In addition, given that cell-based inhibition assays are inherently obscured by nonspecific toxicity, we decided to independently perform the CellTiter-Glo assay for high stringency of selection against cytotoxic compounds.[13]

To validate the biological relevance of the orthogonal reporter assays, we employed siRNA-induced depletion of the transcription factor Sox10 involved in Pmp22 activation in S16 cells.[6] Specific downregulation of the reporters, compared to the control siRNA and also warranted by unaffected cell viability in parallel, indicates that the orthogonal assays properly serve to recapitulate Pmp22 expression (Figure 1B).

Assay Miniaturization for qHTS. qHTS provides concentration response profiles of a chemical library directly from an initial primary screen and thus has advantages over traditional schemes that test each library member at a single concentration. Therefore, we optimized our assays for qHTS in a 1536-well plate format employing 8 titration points (Supplementary Table 1−3) to reduce false positives and enhance the detection of compounds with lower intrinsic or apparent potency.[14] For the screen against the NCGC pharmaceutical collection of approximately 3,000 approved drugs,[15] the orthogonal FLuc and *β*Lac assays were conducted with reporter enzyme inhibitors, *i.e.*, PTC124 and potassium clavulanate, respectively, as positive controls.[16,17] Direct reporter inhibition was intended to biochemically model the relevant range of biological modulation of Pmp22 expression examined in the assays. The CellTiter-Glo viability assay was

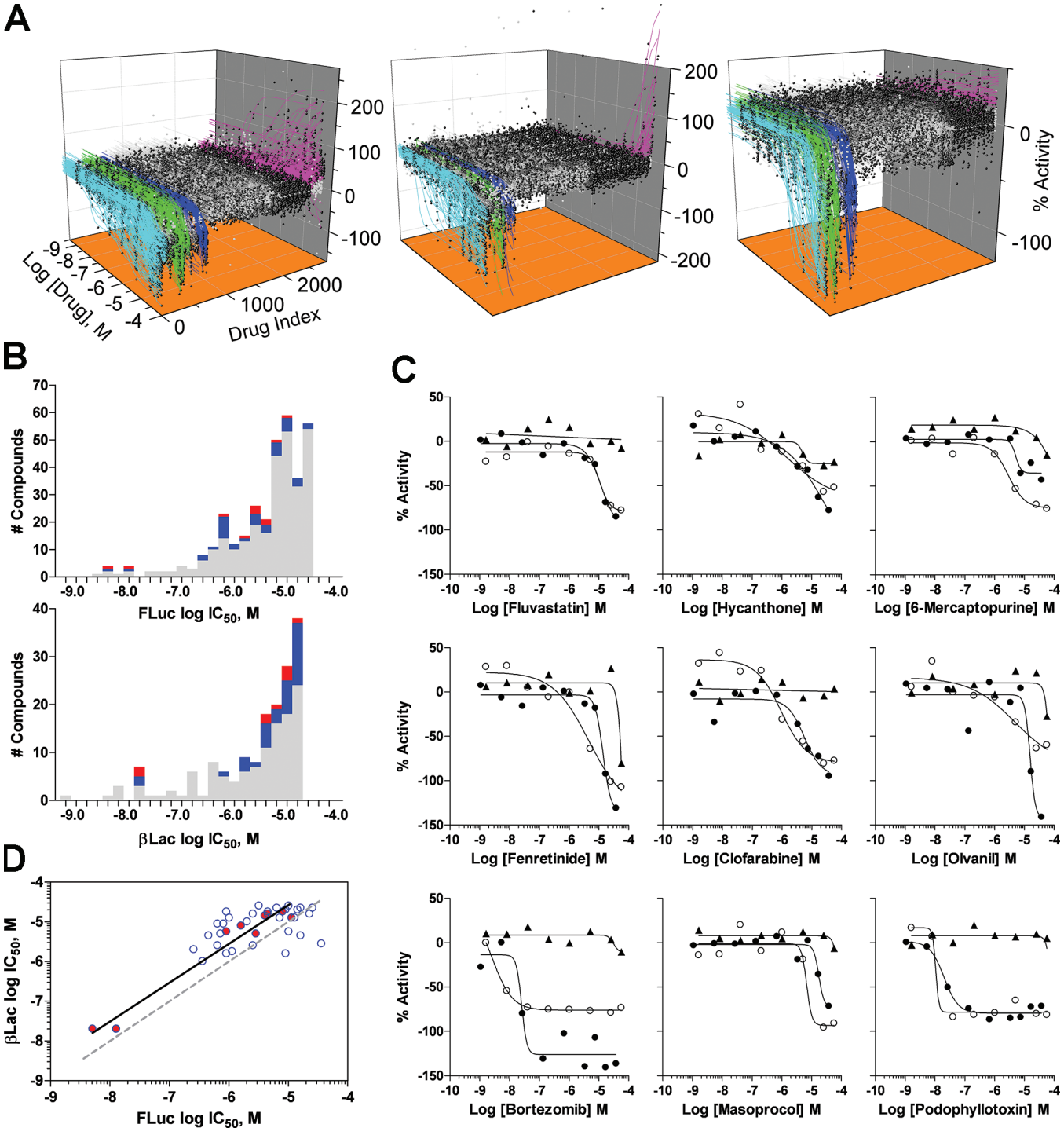

Figure 2. qHTS profiles and active compound selection. (A) 3D plots from qHTS in the FLuc assay, the *β*Lac assay (fluorescence at 460 nm), and CellTiter-Glo assay. CRCs are colored according to curve classification defined in Supplementary Figure 1: light blue (class 1), green (class 2), dark blue (class 3), gray (class 4), and magenta (stimulatory). (B) Top panel: potency distribution of compounds identified in the FLuc assay. Gray bars: the total number of actives identified, blue: concordant actives in the FLuc and *β*Lac assays, red: concordant actives with no significant cytotoxicity. Bottom panel: potency distribution of compounds identified in the *β*Lac assay. Gray bars: the total number of actives identified, blue: concordant actives in the FLuc and *β*Lac assays, red: concordant actives with no significant cytotoxicity. (C) Activity plots of the 9 active compounds in FLuc (○), *β*Lac (●), and CellTiter-Glo (▲) assays. (D) Potency correlation of the 9 actives (solid circles) from the qHTS assays was indicated by the experimental R^2 (a solid line) versus the ideal R^2 of 1 (a dotted line). Open circles represent compounds that are active in both FLuc and *β*Lac (460 nm) assays but cytotoxic in the CellTiter-Glo assay. The data from these screens have been deposited into PubChem Summary AID no. 624036.

normalized to a media-only (no cells) control. The assay performances were adequately sensitive and reproducible as indicated by statistical measures for qHTS (Supplementary Table 4). We note that Z′ values in some of these assays were lower than 0.5, a typical threshold for traditional HTS.[18] However, Z′ values are insufficient to fully reflect the reliability of assay designs that incorporate an additional pharmacological variable as a test of output as opposed to single-point variability.

dx.doi.org/10.1021/cb300048d | *ACS Chem. Biol.* 2012, 7, 1205−1213

Table 1. Orthogonal Cross-Validation Selection Strategy

		compounds			
stage	assay	tested	pass criteria		selection criteria[a]
qHTS	S16 FLuc	2,816	291	10.3%	CC = −la, −lb, and −2a
			175	**6.2%**	inhibitory efficacy >70%
	S16 βLac	2,816	144	5.1%	CC = −la, −lb, −2a, and −2b at 460 nm
			119	**4.2%**	CC ≠ inhibitory CC at 535 nm
	orthoganol cross-validation		**34**	**1.2%**	intersection of FLuc and βLac
	S16 viability	2,816	9	0.3%	CC ≠ −1a, −1b and −2a (counter screen for acute cytotoxicity for 34 cross-validated actives)
secondary	RT-qPCR analysis	9	4	44%	>60% ↓ Pmp22 mRNA expression
	Western analysis	4	3[b]	75%	downregulation of Pmp22 protein; include additional chemotype/class members[c]

[a]CC = curve class. [b]Hycanthone not available for the analysis. [c]Additional proteasome inhibitors added to further explore drug class.

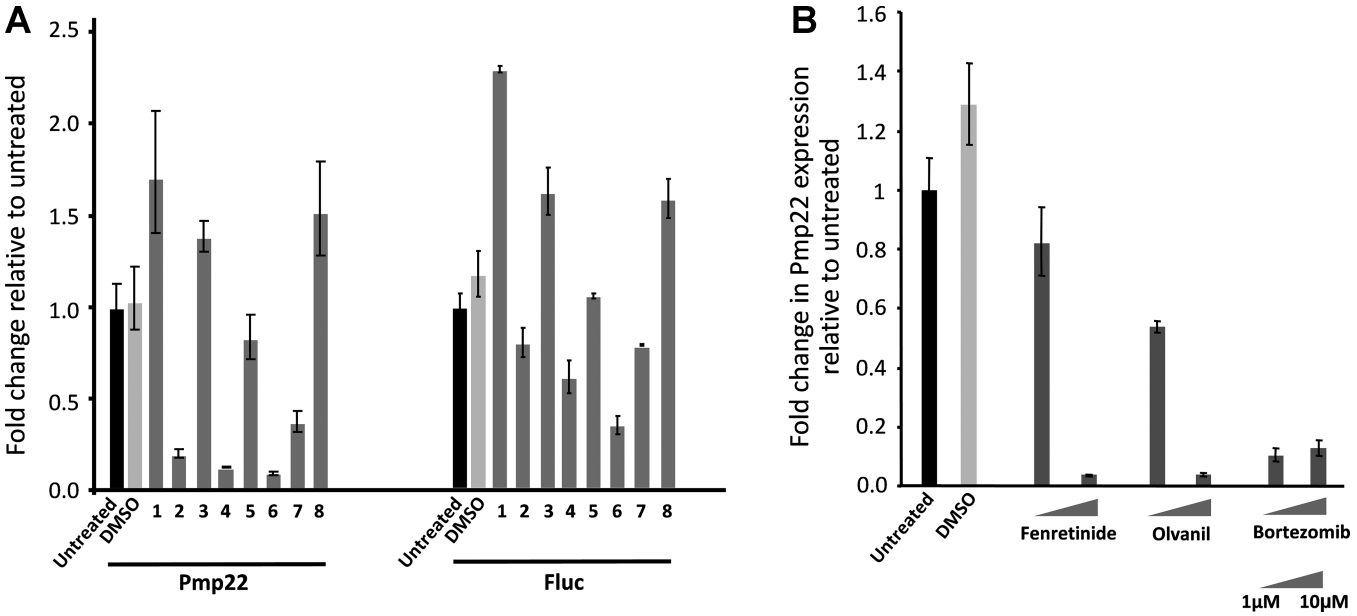

Figure 3. Transcription of endogenous Pmp22 is negatively modulated by actives from qHTS. The FLuc-expressing S16 cells were treated with either DMSO as a control or each compound indicated (1 Fluvastatin; 2 Hycanthone; 3 6-Mercaptopurine; 4 Fenretinide; 5 Clofarabine; 6 Olvanil; 7 Bortezomib; 8 Masoprocol) at 10 μM for 24 h and then subjected to quantitative reverse transcriptase-PCR (RT-qPCR) with primers specific to endogenous Pmp22 or FLuc (A). Similar results were observed with Pmp22 and βLac in the βLac-expressing S16 cells (data not shown). Primary rat Schwann cells were cultured and treated with each drug as described in the Supporting Information before subjected to RT-qPCR for Pmp22 expression analysis (B). Data were first normalized to β-actin (ActB) used as an endogenous loading control across samples and then plotted relative to the untreated sample set to 1 for each target gene. Error bars indicate the SD of three replicates.

On the other hand, MSR values, the minimum potency ratio between two measurements having statistical significance, are more relevant to titration-based screening[19] and indicated acceptable variance to ensure reliable estimates of concentration response relationships obtained from our cell-based qHTS.

Selection and Prioritization of Actives. The activity of compounds was plotted over the concentration range represented by the 8 titration points, generating a single concentration−response curve (CRC) per compound in each assay (Figure 2A). The curves were categorized into three conceptual types (inhibitory, stimulatory, and inactive) and further classified on the basis of efficacy (response magnitude), the number of asymptotes, and quality of fit of the curve to the data (r^2)[14] (Supplementary Figure 1).

To identify compounds mediating inhibition of Pmp22, we first selected the high quality inhibitory curve classes (CCs) representing ∼10% and ∼5% of activity from the FLuc and βLac (fluorescence at 460 nm) assays, respectively (Table 1 and Figure 2B). A total of 175 compounds of inhibitory response greater than 70% were prioritized from the initial 291 actives in the FLuc assay and subsequently cross-referenced with 119 actives from the βLac assay refined by the internal viability FRET (535 nm), which contributed to elimination of inhibitory, thus presumably cytotoxic, compounds. This pairwise juxtaposition of the orthogonal data effectively yielded 34 compounds that exhibited concordant activity in both FLuc and βLac (460 nm) assays. The utility of the CellTiter-Glo assay, introduced as an additional viability screen, was substantiated by the invalidation of additional toxic compounds that evaded the built-in counter-FRET measurement of the βLac assay. Nine compounds were identified to inhibit expression of both FLuc and βLac derived from the *PMP22* intronic element, apparently devoid of nonspecific activity attributed to cytotoxicity and reporter interference (Figure 2C and Supplementary Figure 2). The activity profiles represented by potencies (IC_{50}) of the 9 compounds were tightly correlated between the two orthogonal assays as indicated by the Pearson

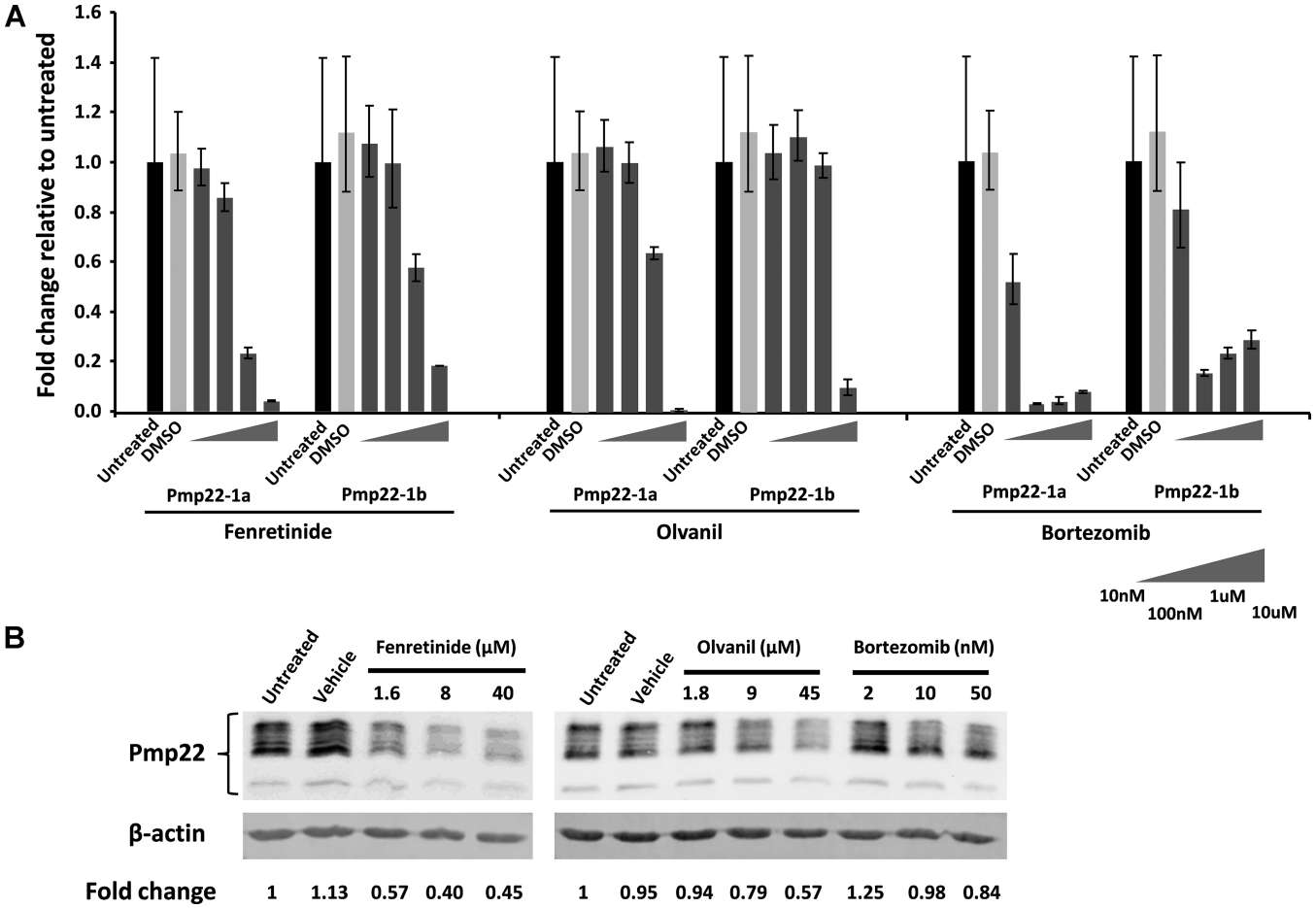

Figure 4. Expression analysis of Pmp22 mRNA transcript variants and protein. The S16 cells were treated with increasing concentrations of each drug for 24 h and then subjected to either RT-qPCR with primers specific to Pmp22-1a and -b (A) or Western blot (B). For mRNA analysis, data were first normalized to ActB used as a loading control across samples and then plotted relative to the untreated sample set to 1 for each target. Error bars indicate the SD of three replicates. For protein analysis, fold change was calculated as a ratio of Pmp22 to β-actin (a loading control) normalized to that of the untreated sample set to 1. Higher concentrations of bortezomib were also tested along with other proteasome inhibitors (Supplementary Figure 7). Vehicles used were ethanol for fenretinide and DMSO for olvanil and bortezomib.

coefficient of R^2 = 0.93 (Figure 2D and Supplementary Table 5). The less sensitive nature of the βLac assay relative to the FLuc assay was also revealed by the displacement of the linear regression by ~8-fold relative to a theoretical fit to assays of equal sensitivity (Figure 2D, dotted line).

Noticeably, in contrast to the βLac assay, there was a preponderance of stimulatory compounds in the FLuc assay (compare left and middle panel in Figure 2A), and 44% (28 out of 63) of them were identified as FLuc enzyme inhibitors in the biochemical FLuc enzyme assay (Supplementary Figure 3). Although seemingly paradoxical, this can be explained by the phenomenon related to the ability of a compound that binds to the FLuc reporter enzyme and stabilizes its cellular half-life.[20] Convincingly, those 28 compounds were also characterized chemically by structures related to known FLuc inhibitors (Supplementary Figure 4).[21]

Conversely, we observed 20 compounds that induced a decrease in the FLuc read-out from the S16 cells but also appeared to be inhibitory in the biochemical FLuc enzyme assay (Supplementary Figure 5). Examination of these compounds revealed that many were complexes with bivalent metal ions (*e.g.*, Hg^{2+}) known to decrease quantum yields and shift spectral output from yellow-green to red of FLuc,[22] while the remainder were highly colored and therefore capable of attenuating bioluminescence through an inner filter effect.[23] It is noteworthy that none of our 9 actives were found in this group of 20 artifact compounds, thus verifying the effectiveness of the orthogonal screen platform in identifying compounds of specific activity.

Inhibition of Endogenous Pmp22 by the Actives Identified. To determine if the 9 actives identified from the reporter-dependent qHTS exhibit physiological effects on Pmp22 expression, quantitative reverse transcriptase (RT)-PCR (qPCR) was utilized to measure the abundance of Pmp22 mRNA transcript in the S16 cells treated with each compound at 10 μM, the concentration point that elicits significant response based on CRCs of the 9 actives profiled in the qHTS. Unexpectedly, podophyllotoxin, one of the 9 actives, led to noticeable cytotoxicity upon visual microscopic inspection and therefore was excluded in subsequent analyses. The specific downregulation of Pmp22 was markedly induced by four drugs (hycanthone, fenretinide, olvanil, and bortezomib), compared to the constitutively active *Gapdh* (glyceraldehyde 3-phosphate dehydrogenase) gene whose expression remained largely unaltered (within the range of 1.3 PCR cycles) across the samples (Figure 3A and Supplementary Figure 6). Similar results were reproduced in primary rat Schwann cells (Figure 3B). Hycanthone, a schistosomicide, was unavailable in a

dx.doi.org/10.1021/cb300048d | *ACS Chem. Biol.* 2012, 7, 1205–1213

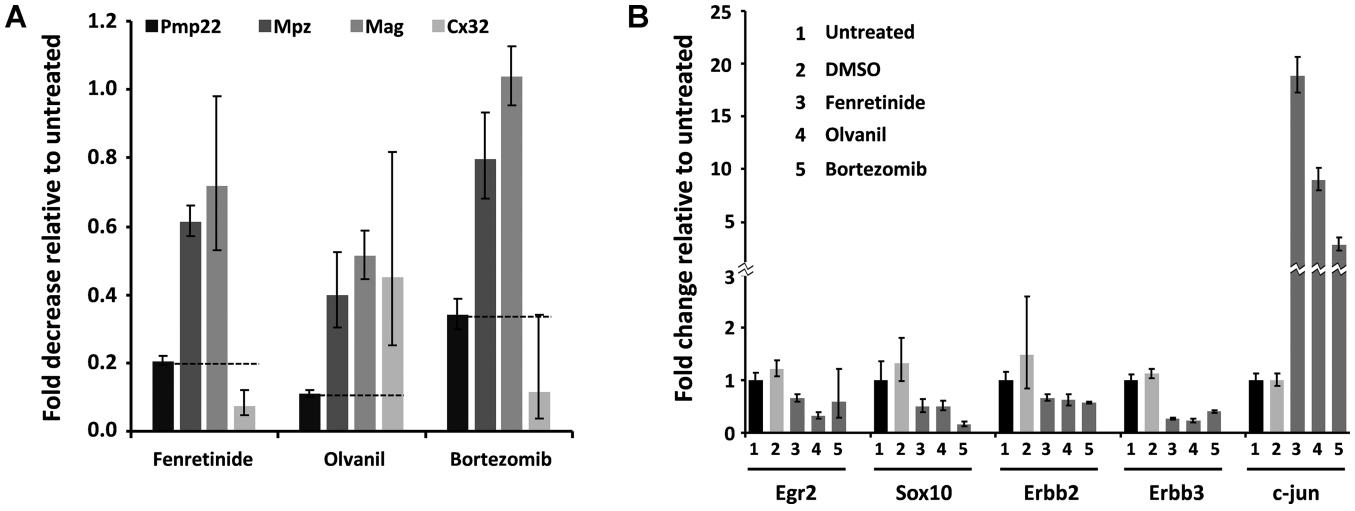

Figure 5. Dynamic changes in expression of myelination regulators. The S16 cells were treated with each drug at 10 μM for 24 h and then applied to RT-qPCR targeting major myelin genes (A) and their regulators (B). Data were first normalized to ActB used as a loading control across samples and then plotted relative to the untreated sample set to 1 for each target gene. Lines are drawn to compare a fold-decrease of Pmp22 with that of the other myelin genes by each drug (A). Error bars indicate the SD of three replicates.

quantity required for subsequent studies. We also introduced FLuc-specific primers to examine how the reporter expression is reflective to that of Pmp22 in the FLuc-expressing S16 cells treated with each compound (Figure 3A). The FLuc expression was consistently repressed, albeit to a lesser degree, which may be explained by different mRNA stability and/or the FLuc reporter regulated solely by the intronic element as opposed to *Pmp22* situated in its entire endogenous locus.

There are two variants of the Pmp22 mRNA transcript (Pmp22-1a and -1b) derived from alternative promoters P1 and P2, respectively.[24] They differ in the first exon but give rise to the identical Pmp22 protein due to the translation initiation site nestled in the second exon shared between the two variants. To dissect the inhibitory regulation of Pmp22 imposed by the three biologically active drugs, variant-specific primer sets were designed for qPCR analysis in the S16 cells treated with an increasing concentration of each drug. All three of the drugs incurred discernibly preferential inhibition toward Pmp22-1a, which is the predominant form of Pmp22 mRNA in myelinating Schwann cells of PNS, whereas Pmp22-1b is expressed in other tissues (Figure 4A).[24]

A surplus of PMP22 protein derived from its gene duplication provides an etiological basis for the phenotypes of CMT1A.[25] Therefore, we further investigated whether the three drugs identified as transcriptional inhibitors for Pmp22 are also capable of modulating the abundance of Pmp22 protein in parallel. The S16 cells treated with a varying concentration of each drug were subjected to Western analysis, which revealed downregulation of Pmp22 protein, albeit less pronounced, consistent with the preceding decrease in Pmp22 mRNA (Figure 4B) and therefore validated the transcription-based assay design for such a dose-sensitive, disease-associated protein as Pmp22. In addition, given that a high turnover of Pmp22 is subject to ubiquitin-dependent degradation,[26] the counter-intuitive decrease of Pmp22 by bortezomib, a proteasome inhibitor, points out an interesting phenomenon of disproportional inhibition of Pmp22 transcription by bortezomib relative to its direct inhibition on the proteasome, which was also observed with other inhibitors in the class (Supplementary Figure 7).

Regulators for Myelination Are Modulated by the Biological Actives. Pmp22 has been known to be dynamically induced along with other myelin genes during postnatal PNS myelination. Therefore, we decided to evaluate the pharmacological specificity of the three drugs toward Pmp22 by qPCR analysis against three major myelin-associated genes: *Mpz* (P_0-Myelin protein zero), *Mag* (Myelin-associated glycoprotein), and *Cx32* (Connexin 32). Overall, all of the three drugs exhibited transcriptional repression across the myelin genes to some extent at the concentration tested (Figure 5A). In particular, *Pmp22* appeared to be most severely inhibited relative to the other myelin genes especially by olvanil, suggesting a titration approach for its enhanced specificity to *Pmp22*. In an attempt to elucidate how the three drugs exert their inhibitory effects on Pmp22, we also sought to examine known regulators involved in PNS myelination. The qPCR analysis unveiled noticeable downregulation of Egr2 and Sox10 as well as Erbb2 and Erbb3,[27−29] which are required for induction of myelination by axonally expressed neuregulin (Figure 5B). Interestingly, Erbb3 has been identified as a target of Sox10 activity.[30] On the other hand, c-jun, a negative regulator for myelination, was significantly upregulated, although Sox2 was unaffected (data not shown).[31,32] With its broad involvement in cellular processes, this upregulation of c-jun could lead to an adverse effect especially in the central nervous system (CNS) where it has been associated with seizures, pain, memory, and stroke.[33] Overall, it is suggested that a reversal of the PNS myelination program is part of the regulatory mechanisms exploited by the three drugs. Additionally, co-titration of combinatorial pairs from the three drugs showed no significant interaction of activity, which suggests they are independently engaged in Pmp22 inhibition (Supplementary Figure 8).

DISCUSSION

Although previous studies have discovered the 5′-flanking region of *Pmp22* involved in Schwann cell-specific expression of Pmp22[5,34] as well as post-transcriptional regulation of Pmp22,[35,36] it still remains elusive how those regulatory pathways specifically converge on PMP22. Due to this limited

dx.doi.org/10.1021/cb300048d | *ACS Chem. Biol.* 2012, 7, 1205−1213

understanding of druggable targets for PMP22 expression, the phenotypic cellular qHTS assays were devised, functionally hinging upon the *PMP22* intronic enhancer, which has been well-characterized to interact with crucial myelin regulators.[6] In addition, the strategic coupling of the phenotypic assays with the NCGC pharmaceutical collection of annotated drugs was intended to provide not only the prospect of drug repurposing for a treatment of CMT1A but also critical insight into the spectrum of PMP22 regulatory circuitry.

The design of the primary orthogonal assays supplemented by the viability screen effectively contributed to the optimal selection and prioritization of actives that were shielded from compound-dependent assay interference.[20] Subsequently, pharmacological activity for endogenous Pmp22 was successfully confirmed in 4 out of the 9 actives identified from the primary qHTS. The cytotoxicity of podophyllotoxin and the confirmation rate of ∼44% (4 out of 9 actives), however, underscore the importance of carefully designed follow-up assays that ascertain biological plausibility of primary qHTS. The interassay (qHTS and follow-up assays) discrepancy observed with the five nonspecific actives cannot be adequately addressed by random integration of the reporters into local chromatin environments that are independent of Pmp22 regulation, since FLuc reporter expression consistently reflected the expression of Pmp22 in the mRNA analysis by qPCR. Rather, while remotely possible, post-translational degradation of the reporters may be facilitated by the drugs, a process that would only be discernible in the primary qHTS assays, not in the follow-up mRNA-based assay. Overall, this discrepancy highlights the challenges in interpreting outcomes of phenotypic assays in primary screening.

One of the Pmp22-modulating drugs, bortezomib, is an anticancer 20S proteasome inhibitor widely used for several neoplasm types including multiple myeloma but accompanied by a dose-limiting adverse effect known as bortezomib-induced peripheral neuropathy (BIPN). Consistent with our findings, the underlying cause of BIPN has been recently illuminated by a perturbation of gene expression in Schwann cells including a decrease in Pmp22,[37] which raises the intriguing possibility of using bortezomib as a Paracelsian small-molecule therapy for treatment of CMT1A. Fenretinide is a synthetic analogue of retinoic acid (RA), and RA has also been implicated in peripheral nerve development, as it dysregulates PNS myelination *via* its differential interaction with retinoic acid receptor (RAR) and retinoid X receptor (RXR).[38] However, due to the complexity of the RA signaling pathway, exemplified by the receptor-independent chemopreventive effect of fenretinide,[39] it remains unclear how fenretinide regulates Pmp22 expression. Olvanil mainly acts as an agonist for the transient receptor potential vanilloid type 1 (TRPV1), a cation channel with high permeability to Ca^{2+}, that mediates thermal nociception and inflammatory pain. Counterintuitively, stimulation of TRPV1 can lead to desensitization of the channel, which is a pharmacological basis for olvanil as an analgesic.[40] The previous report that an abnormal influx of Ca^{2+} facilitated by the purinergic receptor P2X7 underpins the pathogenesis of CMT1A suggests that the activity of Ca^{2+} channels such as TRPV1 modulated by olvanil may be associated with PMP22-sensitive neuropathy.[41] It is revealing that target-centric reassessment of the qHTS led to a group of drugs associated with the TRP superfamily among which capsaicin and camphor displayed inhibitory activity to some extent as well (Supplementary Figure 9). Their disqualification was largely attributed to the stringency of the cross-validating system of the orthogonal assays, which can be technically susceptible to false negatives when one of the assays is of lower sensitivity (*e.g.*, βLac assay) and compound potency is low or solubility-limited. It is also interesting that enhanced activity of TRPV4 caused by genetic mutations has been causatively linked with another type of CMT (CMT type 2C), suggesting a common physiological denominator for CMT pathology.[42] It is notable that our screen did not identify ascorbic acid or progesterone antagonists. However, rodent studies suggest that the ascorbic acid must be used at very high levels to achieve an effect *in vivo*. In addition, it is possible that other regulatory elements in the *Pmp22* gene may mediate the effect of progesterone.

Conclusion. Genomic copy number variation (CNV) provides a basis for genetic predisposition to a range of human diseases.[43] In particular, pathogenetic gene duplications involve dosage-sensitive genes such as *PMP22* for CMT1A, *SNCA* for Parkinson's disease, and *APP* for Alzheimer's disease.[44] Oftentimes, the scarcity of knowledge of molecular targets involved in expression of affected genes hampers drug discovery efforts for associated diseases. The successful use of the phenotypic transcription-based assays described here lays the foundation for qHTS as an enabling resource not only to identify active compounds but also to help unravel a nexus of regulatory pathways so that a rational therapeutic approach can be further developed to pave a new avenue for treatments of genetic disorders. Moreover, translatability of qHTS to human therapeutics can be subsequently assessed by relevant models such as human (patient)-derived Schwann cells including iPSCs (induced pluripotent stem cells) for CMT1A as we deepen our understanding for sophistication of Schwann cell biology.

METHODS

Reporter Constructs and Stable Cell Lines. The *PMP22* intronic element (the coordinates 15,091,959−15,092,201 from human chromosome 17-hg18Mar.2006 build in UCSC Genome Browser) was conjugated upstream of either firefly luciferase (pGL3 luciferase, Promega) or β-lactamase along with the minimal E1B TATA promoter. An IRES Neomycin cassette from the pEFIRES-N plasmid was inserted downstream of the reporter genes. Stable cell line development with the reporter constructs and cell culture conditions are described in the Supporting Information.

Approved Drug Collection. The NCGC pharmaceutical collection (NPC) contained 2816 pharmacologically active drugs at the time of screening.[15] Details on this collection and preparation for testing are described in the Supporting Information.

Reporter Gene and CellTiter-Glo Assays. Assay protocols for qHTS (firefly luciferase, β-lactamase, and CellTiter-Glo assays) are outlined in the Supporting Information.

Data Analysis for qHTS. Data from each assay were normalized plate-wise to corresponding intraplate controls as described previously,[14] see the Supporting Information for additional details.

siRNA Transfection. A 1.5 μg sample of either Sox10-siRNA targeted to: (CAGCGATACCTTAATAAAGTA, cat. no. SI01429351, Qiagen) or a nontargeting (NT) siRNA control (cat. no. 1027280, Qiagen) was transiently transfected into 10^6 FLuc- or βLac-expressing S16 cells using T-020 program of the Amaxa system (Lonza) in the rat neuron nucleofection solution (cat. no. VPG-1003) according to a manufacturer's protocol. The cells were dispensed in 1536-well plates (500 cells per well) using a BioRAPTR FRD and incubated for 48 h before being subjected to assays.

Quantitative Reverse Transcription-PCR Analysis. Quantitative PCR was performed in either SYBR green-based reactions or Taqman-based customized 384-well micro fluidic arrays using a ViiA7 system (Applied biosystems). More details including primer sequences are available in the Supporting Information.

Western Blot Bnalysis. Cells were plated in 6-well plates and treated with each compound at concentrations indicated. After 24 h, lysates were harvested and analyzed by immunoblotting for PMP22 (1:1000, cat. no. ab61220, Abcam) and β-actin (1:1000, cat. no. ab8226, Abcam) as described previously.[6] The membranes were probed with DyLight 800 and 680 conjugated secondary antibodies (1:10,000, cat. nos. 35571 and 35518, Pierce) and imaged using a LiCor Odyssey scanner.

■ ASSOCIATED CONTENT

Supporting Information

This material is available free of charge *via* the Internet at http://pubs.acs.org.

■ AUTHOR INFORMATION

Corresponding Author

*E-mail: jinglese@mail.nih.gov.

Notes

The authors declare no competing financial interest.

■ ACKNOWLEDGMENTS

We thank E. A. Jones, R. Srinivasan, P. Dranchak, and J. Moran for their assistance with cloning, cell line development, and supplementary data. We also thank M. Shen, R. Guha, and P. Shinn for technical data analysis and compound management. Finally, we are indebted to D. S. Auld, S. S. Scherer, and M. E. Shy for insightful discussions and critical comments on the manuscript. This work was supported by grants from the Charcot-Marie-Tooth Association (J.I. and J.S.), NIH Grant R21 NS073726 to J.S., and the NIH Roadmap for Medical Research (J.I.).

■ REFERENCES

(1) Garbay, B., Heape, A. M., Sargueil, F., and Cassagne, C. (2000) Myelin synthesis in the peripheral nervous system. *Prog. Neurobiol. 61*, 267−304.

(2) Reilly, M. M., Murphy, S. M., and Laura, M. (2011) Charcot-Marie-Tooth disease. *J. Peripher. Nerv. Syst. 16*, 1−14.

(3) Robertson, A. M., Perea, J., McGuigan, A., King, R. H., Muddle, J. R., Gabreels-Festen, A. A., Thomas, P. K., and Huxley, C. (2002) Comparison of a new pmp22 transgenic mouse line with other mouse models and human patients with CMT1A. *J. Anat. 200*, 377−390.

(4) Chance, P. F., Alderson, M. K., Leppig, K. A., Lensch, M. W., Matsunami, N., Smith, B., Swanson, P. D., Odelberg, S. J., Disteche, C. M., and Bird, T. D. (1993) DNA deletion associated with hereditary neuropathy with liability to pressure palsies. *Cell 72*, 143−151.

(5) Orfali, W., Nicholson, R. N., Guiot, M. C., Peterson, A. C., and Snipes, G. J. (2005) An 8.5-kb segment of the PMP22 promoter responds to loss of axon signals during Wallerian degeneration, but does not respond to specific axonal signals during nerve regeneration. *J. Neurosci. Res. 80*, 37−46.

(6) Jones, E. A., Lopez-Anido, C., Srinivasan, R., Krueger, C., Chang, L. W., Nagarajan, R., and Svaren, J. (2011) Regulation of the PMP22 gene through an intronic enhancer. *J. Neurosci. 31*, 4242−4250.

(7) Passage, E., Norreel, J. C., Noack-Fraissignes, P., Sanguedolce, V., Pizant, J., Thirion, X., Robaglia-Schlupp, A., Pellissier, J. F., and Fontes, M. (2004) Ascorbic acid treatment corrects the phenotype of a mouse model of Charcot-Marie-Tooth disease. *Nat. Med. 10*, 396−401.

(8) Kaya, F., Belin, S., Bourgeois, P., Micaleff, J., Blin, O., and Fontes, M. (2007) Ascorbic acid inhibits PMP22 expression by reducing cAMP levels. *Neuromuscular Disord. 17*, 248−253.

(9) Pareyson, D., Reilly, M. M., Schenone, A., Fabrizi, G. M., Cavallaro, T., Santoro, L., Vita, G., Quattrone, A., Padua, L., Gemignani, F., Visioli, F., Laura, M., Radice, D., Calabrese, D., Hughes, R. A., and Solari, A. (2011) Ascorbic acid in Charcot-Marie-Tooth disease type 1A (CMT-TRIAAL and CMT-TRAUK): a double-blind randomised trial. *Lancet Neurol. 10*, 320−328.

(10) Sereda, M. W., Meyer zu Horste, G., Suter, U., Uzma, N., and Nave, K. A. (2003) Therapeutic administration of progesterone antagonist in a model of Charcot-Marie-Tooth disease (CMT-1A). *Nat. Med. 9*, 1533−1537.

(11) Hai, M., Muja, N., DeVries, G. H., Quarles, R. H., and Patel, P. I. (2002) Comparative analysis of Schwann cell lines as model systems for myelin gene transcription studies. *J. Neurosci. Res. 69*, 497−508.

(12) Zlokarnik, G. (2000) Fusions to beta-lactamase as a reporter for gene expression in live mammalian cells. *Methods Enzymol. 326*, 221−244.

(13) Crouch, S. P., Kozlowski, R., Slater, K. J., and Fletcher, J. (1993) The use of ATP bioluminescence as a measure of cell proliferation and cytotoxicity. *J. Immunol. Methods 160*, 81−88.

(14) Inglese, J., Auld, D. S., Jadhav, A., Johnson, R. L., Simeonov, A., Yasgar, A., Zheng, W., and Austin, C. P. (2006) Quantitative high-throughput screening: a titration-based approach that efficiently identifies biological activities in large chemical libraries. *Proc. Natl. Acad. Sci. U.S.A. 103*, 11473−11478.

(15) Huang, R., Southall, N., Wang, Y., Yasgar, A., Shinn, P., Jadhav, A., Nguyen, D. T., and Austin, C. P. (2011) The NCGC pharmaceutical collection: a comprehensive resource of clinically approved drugs enabling repurposing and chemical genomics. *Sci. Transl. Med. 3*, 80ps16.

(16) Auld, D. S., Lovell, S., Thorne, N., Lea, W. A., Maloney, D. J., Shen, M., Rai, G., Battaile, K. P., Thomas, C. J., Simeonov, A., Hanzlik, R. P., and Inglese, J. (2010) Molecular basis for the high-affinity binding and stabilization of firefly luciferase by PTC124. *Proc. Natl. Acad. Sci. U.S.A. 107*, 4878−4883.

(17) Reading, C., and Cole, M. (1977) Clavulanic acid: a beta-lactamase-inhiting beta-lactam from Streptomyces clavuligerus. *Antimicrob. Agents Chemother. 11*, 852−857.

(18) Zhang, J. H., Chung, T. D., and Oldenburg, K. R. (1999) A simple statistical parameter for use in evaluation and validation of high throughput screening assays. *J. Biomol. Screening 4*, 67−73.

(19) Eastwood, B. J., Farmen, M. W., Iversen, P. W., Craft, T. J., Smallwood, J. K., Garbison, K. E., Delapp, N. W., and Smith, G. F. (2006) The minimum significant ratio: a statistical parameter to characterize the reproducibility of potency estimates from concentration-response assays and estimation by replicate-experiment studies. *J. Biomol. Screening 11*, 253−261.

(20) Thorne, N., Auld, D. S., and Inglese, J. (2010) Apparent activity in high-throughput screening: origins of compound-dependent assay interference. *Curr. Opin. Chem. Biol. 14*, 315−324.

(21) Auld, D. S., Thorne, N., Nguyen, D. T., and Inglese, J. (2008) A specific mechanism for nonspecific activation in reporter-gene assays. *ACS Chem. Biol. 3*, 463−470.

(22) Wang, Y., Kubota, H., Yamada, N., Irie, T., and Akiyama, H. (2011) Quantum yields and quantitative spectra of firefly bioluminescence with various bivalent metal ions. *Photochem. Photobiol. 87*, 846−852.

(23) Inglese, J., Johnson, R. L., Simeonov, A., Xia, M., Zheng, W., Austin, C. P., and Auld, D. S. (2007) High-throughput screening assays for the identification of chemical probes. *Nat. Chem. Biol. 3*, 466−479.

(24) Suter, U., Snipes, G. J., Schoener-Scott, R., Welcher, A. A., Pareek, S., Lupski, J. R., Murphy, R. A., Shooter, E. M., and Patel, P. I. (1994) Regulation of tissue-specific expression of alternative peripheral myelin protein-22 (PMP22) gene transcripts by two promoters. *J. Biol. Chem. 269*, 25795−25808.

(25) Fortun, J., Go, J. C., Li, J., Amici, S. A., Dunn, W. A., Jr., and Notterpek, L. (2006) Alterations in degradative pathways and protein aggregation in a neuropathy model based on PMP22 overexpression. *Neurobiol. Dis. 22*, 153−164.

(26) Notterpek, L., Ryan, M. C., Tobler, A. R., and Shooter, E. M. (1999) PMP22 accumulation in aggresomes: implications for CMT1A pathology. *Neurobiol. Dis. 6*, 450−460.

(27) Newbern, J., and Birchmeier, C. (2010) Nrg1/ErbB signaling networks in Schwann cell development and myelination. *Semin. Cell Dev. Biol. 21*, 922−928.
(28) Topilko, P., Schneider-Maunoury, S., Levi, G., Baron-Van Evercooren, A., Chennoufi, A. B., Seitanidou, T., Babinet, C., and Charnay, P. (1994) Krox-20 controls myelination in the peripheral nervous system. *Nature 371*, 796−799.
(29) Britsch, S., Goerich, D. E., Riethmacher, D., Peirano, R. I., Rossner, M., Nave, K. A., Birchmeier, C., and Wegner, M. (2001) The transcription factor Sox10 is a key regulator of peripheral glial development. *Genes Dev. 15*, 66−78.
(30) Prasad, M. K., Reed, X., Gorkin, D. U., Cronin, J. C., McAdow, A. R., Chain, K., Hodonsky, C. J., Jones, E. A., Svaren, J., Antonellis, A., Johnson, S. L., Loftus, S. K., Pavan, W. J., and McCallion, A. S. (2011) SOX10 directly modulates ERBB3 transcription via an intronic neural crest enhancer. *BMC Dev. Biol. 11*, 40.
(31) Le, N., Nagarajan, R., Wang, J. Y., Araki, T., Schmidt, R. E., and Milbrandt, J. (2005) Analysis of congenital hypomyelinating Egr2Lo/Lo nerves identifies Sox2 as an inhibitor of Schwann cell differentiation and myelination. *Proc. Natl. Acad. Sci. U.S.A. 102*, 2596−2601.
(32) Parkinson, D. B., Bhaskaran, A., Arthur-Farraj, P., Noon, L., Woodhoo, A., Lloyd, A. C., Feltri, M. L., Wrabetz, L., Behrens, A., Mirsky, R., and Jessen, K. R. (2008) c-Jun is a negative regulator of myelination. *J. Cell Biol. 181*, 625−637.
(33) Raivich, G., and Behrens, A. (2006) Role of the AP-1 transcription factor c-Jun in developing, adult and injured brain. *Prog. Neurobiol. 78*, 347−363.
(34) Maier, M., Berger, P., Nave, K. A., and Suter, U. (2002) Identification of the regulatory region of the peripheral myelin protein 22 (PMP22) gene that directs temporal and spatial expression in development and regeneration of peripheral nerves. *Mol. Cell. Neurosci. 20*, 93−109.
(35) Verrier, J. D., Lau, P., Hudson, L., Murashov, A. K., Renne, R., and Notterpek, L. (2009) Peripheral myelin protein 22 is regulated post-transcriptionally by miRNA-29a. *Glia 57*, 1265−1279.
(36) Bosse, F., Brodbeck, J., and Muller, H. W. (1999) Post-transcriptional regulation of the peripheral myelin protein gene PMP22/gas3. *J. Neurosci. Res. 55*, 164−177.
(37) Shin, Y. K., Jang, S. Y., Lee, H. K., Jung, J., Suh, D. J., Seo, S. Y., and Park, H. T. (2010) Pathological adaptive responses of Schwann cells to endoplasmic reticulum stress in bortezomib-induced peripheral neuropathy. *Glia 58*, 1961−1976.
(38) Latasa, M. J., Ituero, M., Moran-Gonzalez, A., Aranda, A., and Cosgaya, J. M. (2010) Retinoic acid regulates myelin formation in the peripheral nervous system. *Glia 58*, 1451−1464.
(39) Sheikh, M. S., Shao, Z. M., Li, X. S., Ordonez, J. V., Conley, B. A., Wu, S., Dawson, M. I., Han, Q. X., Chao, W. R., Quick, T., Niles, R. M., and Fontana, J. A. (1995) N-(4-Hydroxyphenyl)retinamide (4-HPR)-mediated biological actions involve retinoid receptor-independent pathways in human breast carcinoma. *Carcinogenesis 16*, 2477−2486.
(40) Dray, A. (1992) Neuropharmacological mechanisms of capsaicin and related substances. *Biochem. Pharmacol. 44*, 611−615.
(41) Nobbio, L., Sturla, L., Fiorese, F., Usai, C., Basile, G., Moreschi, I., Benvenuto, F., Zocchi, E., De Flora, A., Schenone, A., and Bruzzone, S. (2009) P2X7-mediated increased intracellular calcium causes functional derangement in Schwann cells from rats with CMT1A neuropathy. *J. Biol. Chem. 284*, 23146−23158.
(42) Landoure, G., Zdebik, A. A., Martinez, T. L., Burnett, B. G., Stanescu, H. C., Inada, H., Shi, Y., Taye, A. A., Kong, L., Munns, C. H., Choo, S. S., Phelps, C. B., Paudel, R., Houlden, H., Ludlow, C. L., Caterina, M. J., Gaudet, R., Kleta, R., Fischbeck, K. H., and Sumner, C. J. (2010) Mutations in TRPV4 cause Charcot-Marie-Tooth disease type 2C. *Nat. Genet. 42*, 170−174.
(43) Fanciulli, M., Petretto, E., and Aitman, T. J. (2009) Gene copy number variation and common human disease. *Clin. Genet. 77*, 201−213.
(44) Conrad, B., and Antonarakis, S. E. (2007) Gene duplication: a drive for phenotypic diversity and cause of human disease. *Annu. Rev. Genomics Hum. Genet. 8*, 17−35.